Constraining the chiral nuclear symmetry energy band with Fermi-energy heavy ion collisions

C Ciampi, S Mallik, F Gulminelli, D Gruyer, J D Frankland, N Le Neindre, R Bougault, A Chbihi, L Baldesi, S Barlini, et al.

Constraining the chiral nuclear symmetry energy band with Fermi-energy heavy ion collisions

C. Ciampi,[1,*] S. Mallik,[2,3,†] F. Gulminelli,[4] D. Gruyer,[4] J. D. Frankland,[1] N. Le Neindre,[4] R. Bougault,[4] A. Chbihi,[1] L. Baldesi,[5,6] S. Barlini,[5,6] B. Borderie,[7] A. Camaiani,[5,6] G. Casini,[5] I. Dekhissi,[4] J. A. Dueñas,[8] Q. Fable,[1] F. Gramegna,[9] M. Henri,[10] B. Hong,[11,12] S. Kim,[13] A. Kordyasz,[14] T. Kozik,[15] I. Lombardo,[16,17] O. Lopez,[4] T. Marchi,[9] S. H. Nam,[11,12] J. Park,[11,12] M. Pârlog,[4,18] G. Pasquali,[5,6] S. Piantelli,[5] G. Poggi,[5,6] S. Valdré,[5] G. Verde,[16,19] and E. Vient[4]

(INDRA-FAZIA collaboration)

[1] *Grand Accélérateur National d'Ions Lourds (GANIL), CEA/DRF–CNRS/IN2P3, Boulevard Henri Becquerel, F-14076 Caen, France*
[2] *Physics Group, Variable Energy Cyclotron Centre, 1/AF Bidhan Nagar, Kolkata 700064, India*
[3] *Homi Bhabha National Institute, Training School Complex, Anushakti Nagar, Mumbai 400085, India*
[4] *Université de Caen Normandie, ENSICAEN, CNRS/IN2P3, LPC Caen UMR6534, F-14000 Caen, France*
[5] *INFN - Sezione di Firenze, 50019 Sesto Fiorentino, Italy*
[6] *Dipartimento di Fisica e Astronomia, Università di Firenze, 50019 Sesto Fiorentino, Italy*
[7] *Université Paris-Saclay, CNRS/IN2P3, IJCLab, 91405 Orsay, France*
[8] *Departamento de Ingeniería Eléctrica y Centro de Estudios Avanzados en Física, Matemáticas y Computación, Universidad de Huelva, 21007 Huelva, Spain*
[9] *INFN - Laboratori Nazionali di Legnaro, 35020 Legnaro, Italy*
[10] *CEA/INSTN/UECC, 143 Chemin de la Crespinière – ZA Les Vindits, F-50130 Cherbourg en Cotentin, France*
[11] *Center for Extreme Nuclear Matters (CENuM), Korea University, Seoul 02841, Republic of Korea*
[12] *Department of Physics, Korea University, Seoul 02841, Republic of Korea*
[13] *Center for Exotic Nuclear Studies, Institute for Basic Science, Daejeon 34126, Republic of Korea*
[14] *Heavy Ion Laboratory, University of Warsaw, 02-093 Warszawa, Poland*
[15] *Marian Smoluchowski Institute of Physics Jagiellonian University, 30-348 Krakow, Poland*
[16] *INFN - Sezione di Catania, 95123 Catania, Italy*
[17] *Dipartimento di Fisica e Astronomia, Università di Catania, via S. Sofia 64, 95123 Catania, Italy*
[18] *"Horia Hulubei" National Institute for R&D in Physics and Nuclear Engineering (IFIN-HH), P. O. Box MG-6, Bucharest Magurele, Romania*
[19] *Laboratoire des 2 Infinis - Toulouse (L2IT-IN2P3), Université de Toulouse, CNRS, UPS, F-31062 Toulouse Cedex 9 (France)*

Heavy ion reactions provide a unique opportunity to unveil the Equation of State (EoS) of baryonic matter in a large density domain. However, to get quantitative constraints it is crucial to employ observables that are as insensitive as possible to final state interaction, and at the same time robustly predicted by transport models with limited model dependence. In this work, we compare for the first time BUU transport calculations to the impact parameter dependence of the isospin transport ratio deduced from INDRA-FAZIA data [1], with a model independent evaluation of the impact parameter. Using different state-of-the-art nuclear functionals, provided both by *ab initio* calculations and by phenomenological approaches, a confidence region for the symmetry energy is extracted. A consistent study of the time dependence of the baryonic density and of the isospin current density allows a precise determination of the density region probed by the experiment. The obtained symmetry energy constraint can be used to inform Bayesian inference of the neutron star EoS.

Heavy-ion collisions (HIC) are unique probes to explore in the laboratory nuclear matter in density conditions different from the one of atomic nuclei at ground state, and can thus potentially bring important constraints to the nuclear Equation of State (EoS) [2], an essential ingredient to the interpretation of gravitational wave data [3]. This is particularly true in the (ultra-) relativistic regime [4], where collective flows and particle production can be compared with transport model calculations in controlled numerical settings [5, 6] to extract the density dependence of the symmetry energy [7] in a density domain lying between the one explored by *ab initio* calculations [8] and nuclear structure experiments [9, 10], and the one probed by astrophysical measurements [11]. Still, the HIC intermediate energy domain provides complementary observables that can meaningfully enrich the available constraints, with the additional advantage that the momentum dependence can still be controlled by the effective mass formalism, and uncertainties on the elementary reaction rates are strongly reduced.

In particular, in Fermi energy HIC, the differential transfer of protons and neutrons between projectile and target, called isospin diffusion, can be measured by the

Isospin Transport Ratio (ITR), defined as [12]:

$$R_i(x) = \frac{2x_i - x_{(A+A)} - x_{(B+B)}}{x_{(A+A)} - x_{(B+B)}}. \quad (1)$$

Here x is an isospin sensitive observable extracted from the final state of reactions between two nuclides A and B, with different neutron-richness, with $i = (A+B), (B+A)$. The value x_i measured for reactions between nuclei with different neutron content is normalized to the reference values obtained when the same nuclide is used for both projectile and target, $(A+A)$ and $(B+B)$. The pioneering works of the MSU group [13] showed that the ITR is strongly correlated to the density dependence of the symmetry energy, allowing the exclusion of extreme values for its magnitude and slope around saturation density ($E_{\rm sym}$ and $L_{\rm sym}$ parameters) [14]. However, to get quantitative constraints, different delicate points need to be addressed: (1) the isospin sensitive observable must be chosen such that it is directly measurable and at the same time robustly predicted by the transport model [15]; (2) the reaction centrality assessment must be reliable and readily comparable between model and data; (3) the density range probed by the ITR in the studied reactions must be estimated to avoid uncontrolled extrapolations.

In this work, we propose significative improvements to all these points. First, the ITR is evaluated using the directly measured neutron to proton ratio of the quasiprojectile remnant [1, 16], a particularly robust observable for the transport models, providing an ITR with very limited sensitivity to secondary decay [17, 18]. This key improvement was possible due to the excellent isotopic identification performance of the FAZIA apparatus [19, 20], able to achieve mass discrimination for heavy nuclei up to $Z \approx 25$. Second, for the centrality assessment we employ a model-independent method to reconstruct the impact parameter distributions contributing to each data point [21]. Finally, for the model comparison we employ functionals extracted from *ab initio* chiral perturbation theory that explore the present uncertainty of the chiral band [22], and we estimate precisely the density associated to the isospin transfer by correlating the time evolution of the isospin current densities [23] and the nuclear density.

We consider ^{58,64}Ni+^{58,64}Ni reactions at 32 MeV/nucleon measured with the INDRA-FAZIA apparatus at GANIL: this dataset has been employed also in Refs. [16, 24], where further experimental details can be found. The experimental data was analyzed [1] with the aim of producing the most model-independent results possible in order to facilitate comparison with the predictions of any transport model. The isospin sensitive observable used to compute the ITR is the average neutron-to-proton ratio $\langle N/Z \rangle$ of the quasiprojectile remnant, identified event-by-event as the forward-emitted fragment with the largest atomic number. The experimental result for the ITR $R(\langle N/Z \rangle)$ as a function

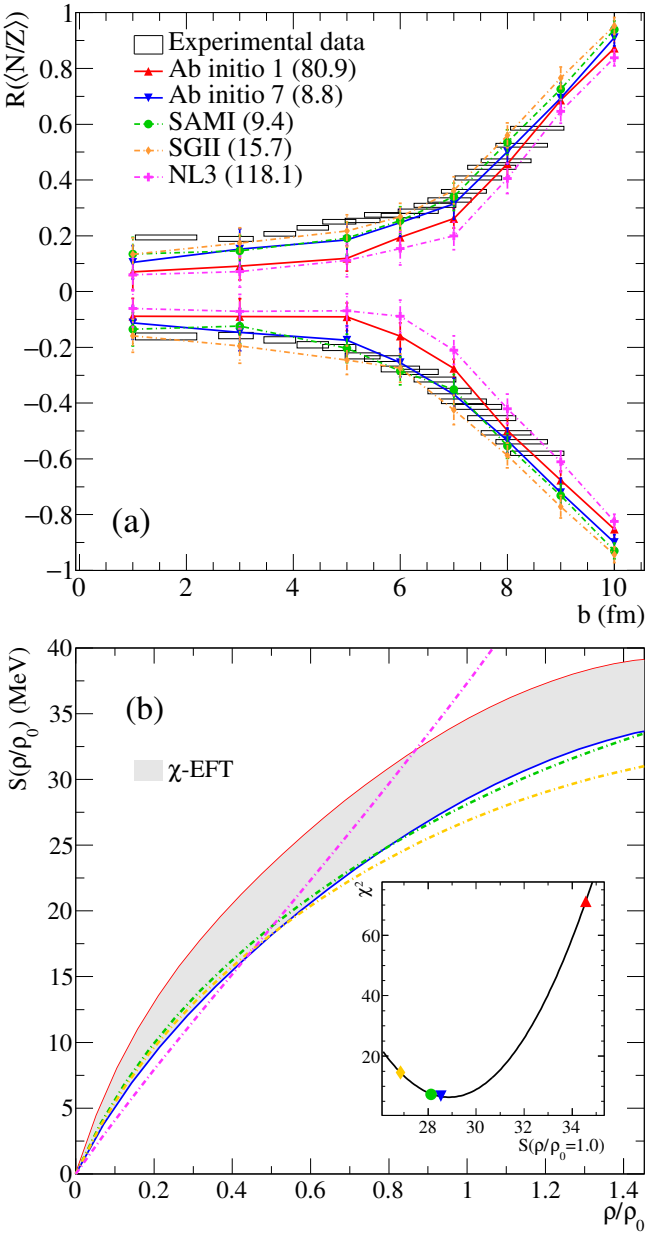

FIG. 1. Impact parameter dependence of the isospin transport ratio R obtained from the $\langle N/Z \rangle$ of quasiprojectile for ^{64}Ni+^{58}Ni and ^{58}Ni+^{64}Ni reactions at 32 MeV/nucleon (a). The experimental results from Ref. [1], shown as open rectangles delimiting the uncertainties, are compared with BUU@VECC-McGill model calculations adopting *ab initio* 1, *ab initio* 7, SAMI, SGII and NL3 EoS parametrizations (lines are drawn to guide the eyes): the corresponding χ^2-values are indicated in parentheses in the legend. The symmetry energy density dependence for the five EoS hereby tested is plotted in (b) using the same color and line-type scheme. Dash-dotted (solid) lines indicate phenomenological (*ab initio*) models. The gray band indicates the uncertainty on the chiral constraint. The inset in (b) shows with a black line the quadratic fit of $\chi^2(S(\rho/\rho_0))$ for $\rho/\rho_0 = 1$, as an example of the procedure.

of the impact parameter b is plotted in Fig. 1(a) with open rectangles [1] representing statistical errors on the y-axis, and the combined effect of statistical errors with those associated with the uncertainties in the b reconstruction procedure [21] along the x-axis.

The theoretical calculations are performed using the BUU@VECC-McGill transport model [25, 26], shown to produce results consistent with similar models in the systematic survey conducted by the Transport Model Evaluation Project (TMEP) [5], both for mean-field [27] and nucleon-nucleon collisions [28]. Ground states of the projectile and target nuclei are constructed with a variational method [29] using Myers density profiles [30]. We use 100 test particles per nucleon. For each reaction, the calculation is carried out for eight impact parameter settings up to the grazing value; for each one of them, 200 events are simulated, due to the long computation time required. The bulk part of the mean-field is calculated from a meta-functional [31] based on a polynomial expansion in density around saturation and including momentum dependence and deviations from the parabolic isospin dependence through the effective mass and its splitting. To cover the present chiral uncertainty on the density dependence of the symmetry energy at sub-saturation, EoS from two extreme χ-EFT interactions (specifically models 1 and 7 in Ref. [22], here abbreviated as *ab initio* 1 and *ab initio* 7, respectively), are considered. The density dependence of the symmetry energy from these two EoS is presented in Fig. 1(b) with solid lines. The gray band of Fig.1(b) thus indicates the present uncertainty on the density dependence of the symmetry energy from nuclear matter *ab initio* calculations [22], and the present challenge from HIC observables is to confirm and possibly reduce this uncertainty band.

Since the chiral perturbation theory becomes less controlled starting from densities of the order of the saturation density ρ_0, we also consider two popular effective models, the relativistic mean-field NL3 [32] and the SGII Skyrme interaction [33], that respect the chiral constraint at low density but correspond to a stiff (respectively, soft) extrapolation for supra-saturation matter. Such relatively extreme behaviors were suggested by analyses of neutron skin measurements [34] and pion production data [35], respectively. The symmetry energy density dependence corresponding to these phenomenological approaches is plotted in Fig. 1(b) with dash-dotted lines. Finally, the Skyrme interaction SAMI [36] is also considered, that corresponds to a symmetry energy behavior almost indistinguishable from *ab initio* 7 but a quite different (and more realistic) behavior for symmetric matter. The comparison between these two models, SAMI and *ab initio* 7, will therefore allow to verify that the adopted observable is indeed suitable to explore isovector properties and is not sensitive to isoscalar ones. For treating finite nuclei, the bulk part is supplemented by a finite range term optimized on nuclear masses [37] as well as Coulomb potential. For more details, we refer the reader to [38].

The ITR predicted by the BUU@VECC-McGill calculations assuming the aforementioned interaction models are displayed in Fig. 1(a), where the same color and line-type scheme as in Fig. 1(b) is employed. In each case, the calculations are run until convergence of the ITR (see Ref. [17]), calculated with the $\langle N/Z \rangle$ of the primary quasiprojectile without secondary de-excitation, thus avoiding possible spurious effects arising from coupling the transport model with an afterburner. The model error bars represent statistical errors due to the finite number of events. The different models here employed fall within the relatively tight limits for the symmetry energy estimated from present constraints (see Fig. 1(b)) and therefore produce similar ITR values, with a similar impact parameter dependence. In particular, we note that the excellent agreement between the *ab initio* 7 and the SAMI results shows that the ITR is indeed probing the density dependence of the symmetry energy.

Figure 1(a) also allows to compare the experimental ITR to those predicted by the BUU code: for reference, χ^2 values resulting from the comparison between experimental data and model predictions for the different EoS here considered are reported in parentheses in the legend. It should be noted that such a comparison is possible thanks to the fact that the ITR strongly suppresses systematic effects in the data such as secondary decay and experimental acceptance [17, 18]. Even if the differences among the theoretical predictions are small, we can still see that the models with the highest symmetry energy around saturation, namely NL3 and *ab initio* 1, can be excluded. Interestingly, this appears to be linked to the absolute value of the symmetry energy above $\approx 0.5\rho_0$, more than to the slope parameter: this already suggests that the collision is probing a density interval close to ρ_0. A global agreement is indeed found among the calculations for SAMI, SGII and *ab initio* 7, all characterized by similar symmetry energy values in this density region: as already evident from Fig. 1(a) and quantitatively expressed by the χ^2 values there reported, the results for these three parametrizations are those providing the most satisfying match of the ITR with the experimental data.

The extracted χ^2 values for the parametrizations under test can be employed to provide approximate confidence regions in the $S - \rho/\rho_0$ plane. To do this, for any given value of ρ/ρ_0, we plotted the χ^2 values corresponding to each functional as a function of their respective $S(\rho/\rho_0)$ values. A parabolic dependence of $\chi^2(S(\rho/\rho_0))$ is observed around its minimum, and such behavior can be extracted by means of a quadratic fit; the result for NL3, giving the worst agreement with the experimental data, has been excluded from the fit procedure. The inset of Fig. 1(b) provides an example showing the quadratic fit for $\rho/\rho_0 = 1$. Assuming Gaussian errors, for each den-

sity we can express the corresponding likelihood function as $\mathcal{L}(S(\rho/\rho_0)) = \mathcal{L}_{\max}(S(\rho/\rho_0)) \exp(-\chi^2(S(\rho/\rho_0))/2)$, which in turn allows to extract the confidence intervals for $S(\rho/\rho_0)$ for various $N\sigma$ confidence levels.

However, the process of isospin diffusion probes the different densities explored by the system with varying sensitivity, which must be accounted for in view of providing a constraint on the symmetry energy density dependence. To this end, further information on the dynamics of this process can be extracted from the BUU@VECC-McGill transport model calculations, in order to define a weight function $w(\rho/\rho_0)$ quantifying the relative influence of each explored density on the observed final isospin equilibration.

We therefore focus on the baryonic density and on the isospin current density. Their time evolution has been extracted and averaged over 200 events for four different impact parameter settings, namely $b = 3$, 5, 7 and 9 fm, assuming an *ab initio* 7 EoS (similar behaviors are obtained for the SAMI EoS). The behavior for intermediate impact parameters has been obtained through interpolation. At each timestep, the baryonic density is calculated within a spherical volume V of radius $r = 3$ fm [39] around the origin of the center of mass frame; its time evolution is shown in Fig. 2(a) for ^{64}Ni+^{58}Ni at 32 MeV/nucleon for a few impact parameters. The isospin current density is defined as $\vec{j}_I = \Delta\vec{j}_n - \Delta\vec{j}_p$, where $\Delta\vec{j}_q = \vec{j}_q^{(P)} + \vec{j}_q^{(T)}$ is the net current density associated to species $q = n, p$ leading to particle exchange from the two colliding nuclei, with:

$$\vec{j}_q^{(X)} = \frac{1}{V}\int_V d^3r \rho_q^{(X)}(\vec{r})\vec{v}_q^{(X)}(\vec{r}). \quad (2)$$

where the local current density is averaged over the same spherical volume V of radius $r = 3$ fm employed for the baryonic density estimation. Here, the local particle density $\rho_q^{(X)}$ and velocity $\vec{v}_q^{(X)}$ is calculated by considering separately the test particles belonging to the projectile (P) and target (T) nucleus before the collision. To follow the dynamics of isospin transfer, the isospin current density must be calculated along the time-dependent principal axis (p.a.), obtained by diagonalizing at each time step the events averaged momentum of inertia tensor:

$$I_{xx} = \sum_{i=1}^{N_{tot}} m\left(y_i^2 + z_i^2\right) \; ; \; I_{zz} = \sum_{i=1}^{N_{tot}} m\left(y_i^2 + x_i^2\right) \; ; \quad (3)$$

$$I_{xz} = -\sum_{i=1}^{N_{tot}} m x_i z_i \; , \quad (4)$$

where m is the nucleon mass, x_i, y_i, z_i are the test particles coordinates and and (x, z) is the reaction plane. The component of the isospin current density along the principal axis $j_{\text{p.a.}}$ is the one contributing to the nucleon exchange between the two colliding nuclei: its time evolution for a few impact parameters is reported in Fig. 2(b) for ^{64}Ni+^{58}Ni at 32 MeV/nucleon, where the positive

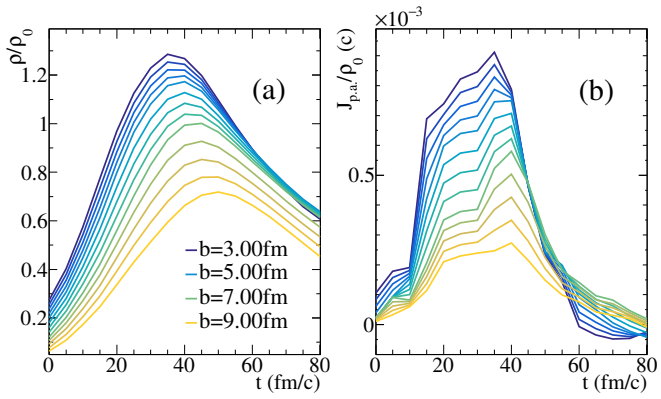

FIG. 2. Time dependence of (a) the baryonic density ρ/ρ_0, (b) the component of the isospin current density along the principal axis $j_{\text{p.a.}}/\rho_0$ for ^{64}Ni+^{58}Ni at 32 MeV/nucleon at different impact parameters between b= 3 fm and 9 fm, obtained from BUU@VECC-McGill calculations with *ab initio* 7 EoS.

sign indicates a net neutron flow from projectile to target leading to isospin equilibration, as expected. It is worth noting that $j_{\text{p.a.}}$ reaches its maximum value when the highest ρ/ρ_0 is reached by the system.

In order to build the weight function $w(\rho/\rho_0)$, we note that the role of each explored density on the final phenomenon depends both on the amount of time spent by the system in that condition, and on the isospin current developing at the same time. Therefore, for a given impact parameter, a partial weight function is extracted by cumulating the baryonic density $\rho(t)/\rho_0$ over time, weighted by the corresponding $j_{\text{p.a.}}(t)$ as follows:

$$w_b(\rho/\rho_0) = \int_{t_{\text{start}}}^{t_{\text{stop}}} j_{\text{p.a.}}(t)\, \delta(\rho/\rho_0 - \rho(t)/\rho_0)\, dt \quad (5)$$

In this work, we integrate between $t_{\text{start}} = 0$ fm/c, corresponding to an initial distance between the projectile and target centers equal to 12 fm, and $t_{\text{stop}} = 80$ fm/c, when there is no further contribution of $j_{\text{p.a.}}$ (see Fig. 2(b)).

To take into account different impact parameters, we integrate the partial weight functions normalized by their integral over the density $\tilde{w}_b(\rho/\rho_0)$ over the selected b-interval:

$$w(\rho/\rho_0) = \int_{b_{\min}}^{b_{\max}} \tilde{w}_b(\rho/\rho_0)\, db \quad (6)$$

Here, we consider impact parameters between 3 fm and 9 fm, where most of the information from the experimental data is concentrated. The likelihood function $\mathcal{L}(S(\rho/\rho_0))$, derived as explained above from the χ^2 values calculated using the experimental ITR data points within this centrality range, is weighted by $w(\rho/\rho_0)$ evaluated over the same interval.

Finally, our constraint for the symmetry energy behavior is shown by means of 1σ (yellow), 2σ (green), 3σ

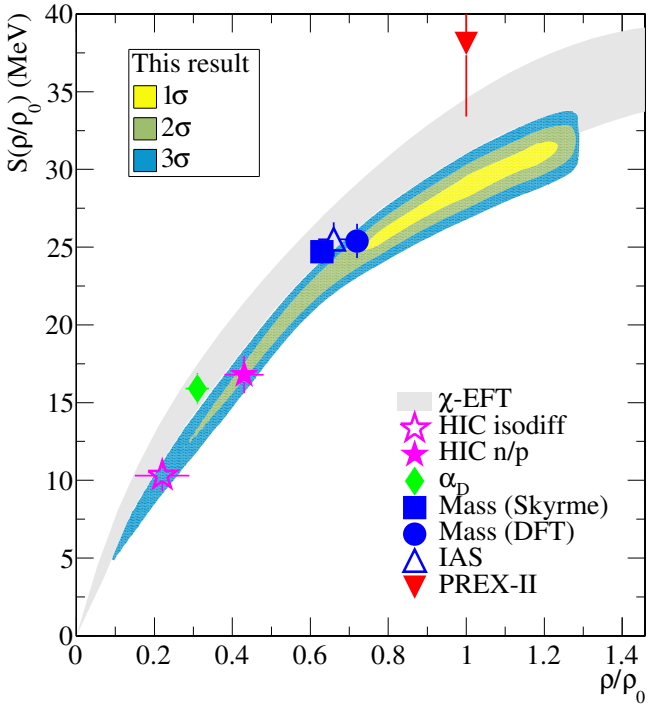

FIG. 3. Constraint on the density dependence of the symmetry energy obtained from this work, represented by the regions in yellow, green and blue corresponding to 1σ, 2σ, 3σ confidence levels respectively. The gray band indicates the uncertainty on the chiral constraint [22]. Markers represent symmetry energy constraints available in the literature [41], extracted from isospin diffusion data in Sn+Sn HIC [42], from single and double ratios of n/p spectra [43], from analyses of nuclear masses [44, 45], isobaric analog states [46] and electric dipole polarizability α_D [47], and from the neutron skin thickness of ^{208}Pb measured by PREX-II [48].

(blue) contours in Fig. 3. Our results are in good agreement with the *ab initio* calculations from Refs. [22, 40] but provide tighter constraints in the probed density region, pointing towards the softer side of the chiral uncertainty band plotted in gray. We stress that in this work, both the extraction of the symmetry energy confidence regions and of the baryonic densities probed via the study of isospin diffusion are treated in a consistent way within the same model framework. Remarkably, the fact that the densities to which the isospin diffusion is most sensitive remain quite close to saturation density allows us to reject stiff behaviors like the one of the NL3 model, behaviors that could not have been discriminated with data probing only densities below $\approx \rho_0/2$. The confidence regions we obtained slightly depend on the considered impact parameter interval: however, our main conclusions are stable against this arbitrary choice. Figure 3 also compares the result hereby presented with the constraints available in the literature [41]. We particularly note a remarkable agreement with previous results obtained from HIC, including isospin diffusion investigations in Sn+Sn systems [42], with the only difference lying in the declared density sensitivity interval.

To conclude, in this work we have confronted the experimentally measured impact parameter dependence of the isospin transport ratio in ^{58,64}Ni+^{58,64}Ni collisions at 32 MeV/nucleon with the predictions of the BUU transport model using state-of-the-art effective nuclear energy density functionals that all respect the present constraints from *ab initio* calculations. A consistent study of the time dependence of the baryonic density and of the isospin current density allows a precise determination of the density region probed by the experiment. Our analysis is in good agreement with the *ab initio* predictions, and produces more stringent constraints on the density dependence of the symmetry energy term of the nuclear equation of state, which can be directly used for the inference of the EoS of astrophysical objects like neutron stars.

Acknowledgments - We acknowledge support from Région Normandie under Réseau d'Intérêt Normand FIDNEOS (RIN/FIDNEOS). This work was supported by the National Research Foundation of Korea (NRF), Grant No. 2018R1A5A1025563 and IBS-R031-D1. Many thanks are due to the accelerator staff of GANIL for delivering a very good quality beam and to the technical staff for the continuous support. S. Mallik acknowledges the GANIL Visiting Scientist program-2023 for very productive stay at Caen. S. Mallik also wishes to thank the VECC C&I Group for providing high-performance computational facilities.

Data availability - The supporting experimental data for this article are from the e789_18 experiment and are registered as [49] following the GANIL Data Policy.

* caterina.ciampi@ganil.fr
† swagato@vecc.gov.in

[1] C. Ciampi, J. D. Frankland, D. Gruyer, N. L. Neindre, S. Mallik, R. Bougault, A. Chbihi, L. Baldesi, S. Barlini, E. Bonnet, B. Borderie, A. Camaiani, G. Casini, I. Dekhissi, D. Dell'Aquila, J. A. Dueñas, Q. Fable, F. Gramegna, C. Gouyet, M. Henri, B. Hong, S. Kim, A. Kordyasz, T. Kozik, M. J. Kweon, I. Lombardo, O. Lopez, L. Manduci, T. Marchi, K. Mazurek, S. H. Nam, J. Park, M. Pârlog, G. Pasquali, S. Piantelli, G. Poggi, A. Rebillard-Soulié, R. Revenko, S. Valdré, G. Verde, and E. Vient, submitted to Phys. Rev. C (2024), arXiv:2412.13648 [nucl-ex].
[2] S. Huth, P. T. H. Pang, I. Tews, T. Dietrich, A. Le Fèvre, A. Schwenk, W. Trautmann, K. Agarwal, M. Bulla, M. W. Coughlin, and C. Van Den Broeck, Nature **606**, 276 (2022).
[3] J. M. Lattimer, Annual Review of Nuclear and Particle Science **71**, 433 (2021).
[4] A. Sorensen, K. Agarwal, K. W. Brown, Z. Chajecki, P. Danielewicz, C. Drischler, S. Gandolfi, J. W. Holt,

M. Kaminski, C.-M. Ko, R. Kumar, B.-A. Li, W. G. Lynch, A. B. McIntosh, W. G. Newton, S. Pratt, O. Savchuk, M. Stefaniak, I. Tews, M. B. Tsang, R. Vogt, H. Wolter, H. Zbroszczyk, N. Abbasi, J. Aichelin, A. Andronic, S. A. Bass, F. Becattini, D. Blaschke, M. Bleicher, C. Blume, E. Bratkovskaya, B. A. Brown, D. A. Brown, A. Camaiani, G. Casini, K. Chatziioannou, A. Chbihi, M. Colonna, M. D. Cozma, V. Dexheimer, X. Dong, T. Dore, L. Du, J. A. Dueñas, H. Elfner, W. Florkowski, Y. Fujimoto, R. J. Furnstahl, A. Gade, T. Galatyuk, C. Gale, F. Geurts, F. Gramegna, S. Grozdanov, K. Hagel, S. P. Harris, W. Haxton, U. Heinz, M. P. Heller, O. Hen, H. Hergert, N. Herrmann, H. Z. Huang, X.-G. Huang, N. Ikeno, G. Inghirami, J. Jankowski, J. Jia, J. C. Jiménez, J. Kapusta, B. Kardan, I. Karpenko, D. Keane, D. Kharzeev, A. Kugler, A. Le Fèvre, D. Lee, H. Liu, M. A. Lisa, W. J. Llope, I. Lombardo, M. Lorenz, T. Marchi, L. McLerran, U. Mosel, A. Motornenko, B. Müller, P. Napolitani, J. B. Natowitz, W. Nazarewicz, J. Noronha, J. Noronha-Hostler, G. Odyniec, P. Papakonstantinou, Z. Paulínyová, J. Piekarewicz, R. D. Pisarski, C. Plumberg, M. Prakash, J. Randrup, C. Ratti, P. Rau, S. Reddy, H.-R. Schmidt, P. Russotto, R. Ryblewski, A. Schäfer, B. Schenke, S. Sen, P. Senger, R. Seto, C. Shen, B. Sherrill, M. Singh, V. Skokov, M. Spaliński, J. Steinheimer, M. Stephanov, J. Stroth, C. Sturm, K.-J. Sun, A. Tang, G. Torrieri, W. Trautmann, G. Verde, V. Vovchenko, R. Wada, F. Wang, G. Wang, K. Werner, N. Xu, Z. Xu, H.-U. Yee, S. Yennello, and Y. Yin, Progress in Particle and Nuclear Physics **134**, 104080 (2024).

[5] H. Wolter, M. Colonna, D. Cozma, P. Danielewicz, C. M. Ko, R. Kumar, A. Ono, M. B. Tsang, J. Xu, Y.-X. Zhang, E. Bratkovskaya, Z.-Q. Feng, T. Gaitanos, A. Le Fèvre, N. Ikeno, Y. Kim, S. Mallik, P. Napolitani, D. Oliinychenko, T. Ogawa, M. Papa, J. Su, R. Wang, Y.-J. Wang, J. Weil, F.-S. Zhang, G.-Q. Zhang, Z. Zhang, J. Aichelin, W. Cassing, L.-W. Chen, H.-G. Cheng, H. Elfner, K. Gallmeister, C. Hartnack, S. Hashimoto, S. Jeon, K. Kim, M. Kim, B.-A. Li, C.-H. Lee, Q.-F. Li, Z.-X. Li, U. Mosel, Y. Nara, K. Niita, A. Ohnishi, T. Sato, T. Song, A. Sorensen, N. Wang, and W.-J. Xie, Progress in Particle and Nuclear Physics **125**, 103962 (2022).

[6] J. Xu, H. Wolter, M. Colonna, M. D. Cozma, P. Danielewicz, C. M. Ko, A. Ono, M. B. Tsang, Y.-X. Zhang, H.-G. Cheng, N. Ikeno, R. Kumar, J. Su, H. Zheng, Z. Zhang, L.-W. Chen, Z.-Q. Feng, C. Hartnack, A. Le Fèvre, B.-A. Li, Y. Nara, A. Ohnishi, and F.-S. Zhang (TMEP Collaboration), Phys. Rev. C **109**, 044609 (2024).

[7] B.-A. Li, L.-W. Chen, and C. M. Ko, Physics Reports **464**, 113 (2008).

[8] J. Carlson, S. Gandolfi, F. Pederiva, S. C. Pieper, R. Schiavilla, K. E. Schmidt, and R. B. Wiringa, Rev. Mod. Phys. **87**, 1067 (2015).

[9] D. Adhikari, H. Albataineh, D. Androic, K. Aniol, D. S. Armstrong, T. Averett, C. Ayerbe Gayoso, S. Barcus, V. Bellini, R. S. Beminiwattha, J. F. Benesch, H. Bhatt, D. Bhatta Pathak, D. Bhetuwal, B. Blaikie, Q. Campagna, A. Camsonne, G. D. Cates, Y. Chen, C. Clarke, J. C. Cornejo, S. Covrig Dusa, P. Datta, A. Deshpande, D. Dutta, C. Feldman, E. Fuchey, C. Gal, D. Gaskell, T. Gautam, M. Gericke, C. Ghosh, I. Halilovic, J.-O. Hansen, F. Hauenstein, W. Henry, C. J. Horowitz, C. Jantzi, S. Jian, S. Johnston, D. C. Jones, B. Karki, S. Katugampola, C. Keppel, P. M. King, D. E. King, M. Knauss, K. S. Kumar, T. Kutz, N. Lashley-Colthirst, G. Leverick, H. Liu, N. Liyange, S. Malace, R. Mammei, J. Mammei, M. McCaughan, D. McNulty, D. Meekins, C. Metts, R. Michaels, M. M. Mondal, J. Napolitano, A. Narayan, D. Nikolaev, M. N. H. Rashad, V. Owen, C. Palatchi, J. Pan, B. Pandey, S. Park, K. D. Paschke, M. Petrusky, M. L. Pitt, S. Premathilake, A. J. R. Puckett, B. Quinn, R. Radloff, S. Rahman, A. Rathnayake, B. T. Reed, P. E. Reimer, R. Richards, S. Riordan, Y. Roblin, S. Seeds, A. Shahinyan, P. Souder, L. Tang, M. Thiel, Y. Tian, G. M. Urciuoli, E. W. Wertz, B. Wojtsekhowski, B. Yale, T. Ye, A. Yoon, A. Zec, W. Zhang, J. Zhang, and X. Zheng (PREX Collaboration), Phys. Rev. Lett. **126**, 172502 (2021).

[10] D. Adhikari, H. Albataineh, D. Androic, K. A. Aniol, D. S. Armstrong, T. Averett, C. Ayerbe Gayoso, S. K. Barcus, V. Bellini, R. S. Beminiwattha, J. F. Benesch, H. Bhatt, D. Bhatta Pathak, D. Bhetuwal, B. Blaikie, J. Boyd, Q. Campagna, A. Camsonne, G. D. Cates, Y. Chen, C. Clarke, J. C. Cornejo, S. Covrig Dusa, M. M. Dalton, P. Datta, A. Deshpande, D. Dutta, C. Feldman, E. Fuchey, C. Gal, D. Gaskell, T. Gautam, M. Gericke, C. Ghosh, I. Halilovic, J.-O. Hansen, O. Hassan, F. Hauenstein, W. Henry, C. J. Horowitz, C. Jantzi, S. Jian, S. Johnston, D. C. Jones, S. Kakkar, S. Katugampola, C. Keppel, P. M. King, D. E. King, K. S. Kumar, T. Kutz, N. Lashley-Colthirst, G. Leverick, H. Liu, N. Liyanage, J. Mammei, R. Mammei, M. McCaughan, D. McNulty, D. Meekins, C. Metts, R. Michaels, M. Mihovilovic, M. M. Mondal, J. Napolitano, A. Narayan, D. Nikolaev, V. Owen, C. Palatchi, J. Pan, B. Pandey, S. Park, K. D. Paschke, M. Petrusky, M. L. Pitt, S. Premathilake, B. Quinn, R. Radloff, S. Rahman, M. N. H. Rashad, A. Rathnayake, B. T. Reed, P. E. Reimer, R. Richards, S. Riordan, Y. R. Roblin, S. Seeds, A. Shahinyan, P. Souder, M. Thiel, Y. Tian, G. M. Urciuoli, E. W. Wertz, B. Wojtsekhowski, B. Yale, T. Ye, A. Yoon, W. Xiong, A. Zec, W. Zhang, J. Zhang, and X. Zheng (CREX Collaboration), Phys. Rev. Lett. **129**, 042501 (2022).

[11] B. P. Abbott, R. Abbott, T. D. Abbott, F. Acernese, K. Ackley, C. Adams, T. Adams, P. Addesso, R. X. Adhikari, V. B. Adya, C. Affeldt, B. Agarwal, M. Agathos, K. Agatsuma, N. Aggarwal, O. D. Aguiar, L. Aiello, A. Ain, P. Ajith, B. Allen, G. Allen, A. Allocca, M. A. Aloy, P. A. Altin, A. Amato, A. Ananyeva, S. B. Anderson, W. G. Anderson, S. V. Angelova, S. Antier, S. Appert, K. Arai, M. C. Araya, J. S. Areeda, *et al.* (LIGO Scientific Collaboration and Virgo Collaboration), Phys. Rev. X **9**, 011001 (2019).

[12] F. Rami, Y. Leifels, B. de Schauenburg, A. Gobbi, B. Hong, J. P. Alard, A. Andronic, R. Averbeck, V. Barret, Z. Basrak, N. Bastid, I. Belyaev, A. Bendarag, G. Berek, R. Čaplar, N. Cindro, P. Crochet, A. Devismes, P. Dupieux, M. Dželalija, M. Eskef, C. Finck, Z. Fodor, H. Folger, L. Fraysse, A. Genoux-Lubain, Y. Grigorian, Y. Grishkin, N. Herrmann, K. D. Hildenbrand, J. Kecskemeti, Y. J. Kim, P. Koczon, M. Kirejczyk, M. Korolija, R. Kotte, M. Kowalczyk, T. Kress, R. Kutsche, A. Lebedev, K. S. Lee, V. Manko, H. Merlitz, S. Mohren, D. Moisa, J. Mösner, W. Neubert, A. Nianine, D. Pelte, M. Petrovici, C. Pinkenburg, C. Plettner,

W. Reisdorf, J. Ritman, D. Schüll, Z. Seres, B. Sikora, K. S. Sim, V. Simion, K. Siwek-Wilczyńska, A. Somov, M. R. Stockmeier, G. Stoicea, M. Vasiliev, P. Wagner, K. Wiśniewski, D. Wohlfarth, J. T. Yang, I. Yushmanov, and A. Zhilin (FOPI Collaboration), Phys. Rev. Lett. **84**, 1120 (2000).

[13] M. B. Tsang, W. A. Friedman, C. K. Gelbke, W. G. Lynch, G. Verde, and H. S. Xu, Phys. Rev. Lett. **86**, 5023 (2001).

[14] M. B. Tsang, J. R. Stone, F. Camera, P. Danielewicz, S. Gandolfi, K. Hebeler, C. J. Horowitz, J. Lee, W. G. Lynch, Z. Kohley, R. Lemmon, P. Möller, T. Murakami, S. Riordan, X. Roca-Maza, F. Sammarruca, A. W. Steiner, I. Vidaña, and S. J. Yennello, Phys. Rev. C **86**, 015803 (2012).

[15] Y. Zhang, D. D. S. Coupland, P. Danielewicz, Z. Li, H. Liu, F. Lu, W. G. Lynch, and M. B. Tsang, Phys. Rev. C **85**, 024602 (2012).

[16] C. Ciampi, S. Piantelli, G. Casini, G. Pasquali, J. Quicray, L. Baldesi, S. Barlini, B. Borderie, R. Bougault, A. Camaiani, A. Chbihi, D. Dell'Aquila, M. Cicerchia, J. A. Dueñas, Q. Fable, D. Fabris, J. D. Frankland, C. Frosin, T. Génard, F. Gramegna, D. Gruyer, M. Henri, B. Hong, S. Kim, A. Kordyasz, T. Kozik, M. J. Kweon, J. Lemarié, N. Le Neindre, I. Lombardo, O. Lopez, T. Marchi, S. H. Nam, A. Ordine, P. Ottanelli, J. Park, J. H. Park, M. Pârlog, G. Poggi, A. Rebillard-Soulié, A. A. Stefanini, S. Upadhyaya, S. Valdré, G. Verde, E. Vient, and M. Vigilante, Physical Review C **106**, 024603 (2022).

[17] S. Mallik, F. Gulminelli, and D. Gruyer, Journal of Physics G: Nuclear and Particle Physics **49**, 015102 (2021).

[18] A. Camaiani, S. Piantelli, A. Ono, G. Casini, B. Borderie, R. Bougault, C. Ciampi, J. A. Dueñas, C. Frosin, J. D. Frankland, D. Gruyer, N. LeNeindre, I. Lombardo, G. Mantovani, P. Ottanelli, M. Parlog, G. Pasquali, S. Upadhyaya, S. Valdré, G. Verde, and E. Vient, Physical Review C **102**, 044607 (2020).

[19] R. Bougault, G. Poggi, S. Barlini, B. Borderie, G. Casini, A. Chbihi, N. Le Neindre, M. Pârlog, G. Pasquali, S. Piantelli, Z. Sosin, G. Ademard, R. Alba, A. Anastasio, S. Barbey, L. Bardelli, M. Bini, A. Boiano, M. Boisjoli, E. Bonnet, R. Borcea, B. Bougard, G. Brulin, M. Bruno, S. Carboni, C. Cassese, F. Cassese, M. Cinausero, L. Ciolacu, I. Cruceru, M. Cruceru, B. D'Aquino, B. D. Fazio, M. Degerlier, P. Desrues, P. D. Meo, J. A. Dueñas, P. Edelbruck, S. Energico, M. Falorsi, J. D. Frankland, E. Galichet, K. Gasior, F. Gramegna, R. Giordano, D. Gruyer, A. Grzeszczuk, M. Guerzoni, H. Hamrita, C. Huss, M. Kajetanowicz, K. Korcyl, A. Kordyasz, T. Kozik, P. Kulig, L. Lavergne, E. Legouée, O. Lopez, J. Łukasik, C. Maiolino, T. Marchi, P. Marini, I. Martel, V. Masone, A. Meoli, Y. Merrer, L. Morelli, F. Negoita, A. Olmi, A. Ordine, G. Paduano, C. Pain, M. Pałka, G. Passeggio, G. Pastore, P. Pawłowski, M. Petcu, H. Petrascu, E. Piasecki, G. Pontoriere, E. Rauly, M. F. Rivet, R. Rocco, E. Rosato, L. Roscilli, E. Scarlini, F. Salomon, D. Santonocito, V. Seredov, S. Serra, D. Sierpowski, G. Spadaccini, C. Spitaels, A. A. Stefanini, G. Tobia, G. Tortone, T. Twaróg, S. Valdré, A. Vanzanella, E. Vanzanella, E. Vient, M. Vigilante, G. Vitiello, E. Wanlin, A. Wieloch, and W. Zipper (the FAZIA collaboration), Eur. Phys. J. A **50**, 47 (2014).

[20] S. Valdré, G. Casini, N. Le Neindre, M. Bini, A. Boiano, B. Borderie, P. Edelbruck, G. Poggi, F. Salomon, G. Tortone, R. Alba, S. Barlini, E. Bonnet, B. Bougard, R. Bougault, G. Brulin, M. Bruno, A. Buccola, A. Camaiani, A. Chbihi, C. Ciampi, M. Cicerchia, M. Cinausero, D. Dell'Aquila, P. Desrues, J. Dueñas, D. Fabris, M. Falorsi, J. Frankland, C. Frosin, E. Galichet, R. Giordano, F. Gramegna, L. Grassi, D. Gruyer, M. Guerzoni, M. Henri, M. Kajetanowicz, K. Korcyl, A. Kordyasz, T. Kozik, P. Lecomte, I. Lombardo, O. Lopez, C. Maiolino, G. Mantovani, T. Marchi, A. Margotti, Y. Merrer, L. Morelli, A. Olmi, A. Ordine, P. Ottanelli, C. Pain, M. Pałka, M. Pârlog, G. Pasquali, G. Pastore, S. Piantelli, H. de Préaumont, R. Revenko, A. Richard, M. Rivet, J. Ropert, E. Rosato, F. Saillant, D. Santonocito, E. Scarlini, S. Serra, C. Soulet, G. Spadaccini, A. Stefanini, G. Tobia, S. Upadhyaya, A. Vanzanella, G. Verde, E. Vient, M. Vigilante, E. Wanlin, G. Wittwer, and A. Zucchini, Nuclear Instruments and Methods in Physics Research Section A: Accelerators, Spectrometers, Detectors and Associated Equipment **930**, 27 (2019).

[21] J. D. Frankland, D. Gruyer, E. Bonnet, B. Borderie, R. Bougault, A. Chbihi, J. E. Ducret, D. Durand, Q. Fable, M. Henri, J. Lemarié, N. Le Neindre, I. Lombardo, O. Lopez, L. Manduci, M. Pârlog, J. Quicray, G. Verde, E. Vient, and M. Vigilante (INDRA Collaboration), Phys. Rev. C **104**, 034609 (2021).

[22] C. Drischler, K. Hebeler, and A. Schwenk, Phys. Rev. C **93**, 054314 (2016).

[23] V. Baran, M. Colonna, V. Greco, and M. Di Toro, Physics Reports **410**, 335 (2005).

[24] C. Ciampi, S. Piantelli, G. Casini, A. Ono, J. D. Frankland, L. Baldesi, S. Barlini, B. Borderie, R. Bougault, A. Camaiani, A. Chbihi, J. A. Dueñas, Q. Fable, D. Fabris, C. Frosin, T. Génard, F. Gramegna, D. Gruyer, M. Henri, B. Hong, S. Kim, A. Kordyasz, T. Kozik, M. J. Kweon, N. Le Neindre, I. Lombardo, O. Lopez, T. Marchi, K. Mazurek, S. H. Nam, J. Park, M. Pârlog, G. Pasquali, G. Poggi, A. Rebillard-Soulié, A. A. Stefanini, S. Upadhyaya, S. Valdré, G. Verde, E. Vient, and M. Vigilante, Physical Review C **108**, 054611 (2023).

[25] S. Mallik, S. Das Gupta, and G. Chaudhuri, Phys. Rev. C **91**, 034616 (2015).

[26] S. Mallik and G. Chaudhuri, Nuclear Physics A **1002**, 121948 (2020).

[27] M. Colonna, Y.-X. Zhang, Y.-J. Wang, D. Cozma, P. Danielewicz, C. M. Ko, A. Ono, M. B. Tsang, R. Wang, H. Wolter, J. Xu, Z. Zhang, L.-W. Chen, H.-G. Cheng, H. Elfner, Z.-Q. Feng, M. Kim, Y. Kim, S. Jeon, C.-H. Lee, B.-A. Li, Q.-F. Li, Z.-X. Li, S. Mallik, D. Oliinychenko, J. Su, T. Song, A. Sorensen, and F.-S. Zhang, Phys. Rev. C **104**, 024603 (2021).

[28] Y.-X. Zhang, Y.-J. Wang, M. Colonna, P. Danielewicz, A. Ono, M. B. Tsang, H. Wolter, J. Xu, L.-W. Chen, D. Cozma, Z.-Q. Feng, S. Das Gupta, N. Ikeno, C.-M. Ko, B.-A. Li, Q.-F. Li, Z.-X. Li, S. Mallik, Y. Nara, T. Ogawa, A. Ohnishi, D. Oliinychenko, M. Papa, H. Petersen, J. Su, T. Song, J. Weil, N. Wang, F.-S. Zhang, and Z. Zhang, Phys. Rev. C **97**, 034625 (2018).

[29] S. J. Lee, H. H. Gan, E. D. Cooper, and S. Das Gupta, Phys. Rev. C **40**, 2585 (1989).

[30] W. D. Myers, Nuclear Physics A **296**, 177 (1978).

[31] J. Margueron, R. Hoffmann Casali, and F. Gulminelli,

Phys. Rev. C **97**, 025805 (2018).
[32] G. A. Lalazissis, J. König, and P. Ring, Phys. Rev. C **55**, 540 (1997).
[33] N. Van Giai and H. Sagawa, Physics Letters B **106**, 379 (1981).
[34] B. T. Reed, F. J. Fattoyev, C. J. Horowitz, and J. Piekarewicz, Phys. Rev. C **109**, 035803 (2024).
[35] Z. Xiao, B.-A. Li, L.-W. Chen, G.-C. Yong, and M. Zhang, Phys. Rev. Lett. **102**, 062502 (2009).
[36] X. Roca-Maza, G. Colò, and H. Sagawa, Phys. Rev. C **86**, 031306 (2012).
[37] R. J. Lenk and V. R. Pandharipande, Phys. Rev. C **39**, 2242 (1989).
[38] S. Mallik, G. Chaudhuri, and F. Gulminelli, Phys. Rev. C **100**, 024611 (2019).
[39] The choice of the $r = 3$ fm radius of the examination sphere represented the optimal trade-off between a clean selection of the contact region and the control of statistical fluctuations due to the finite number of test particles within V. For a ± 0.5 fm variation of such radius, we observe a corresponding percentage variation on $\rho(t)$ between 2% and 5%, leading to very minor differences on the weight function and hence on our final constraint.
[40] S. Huth, C. Wellenhofer, and A. Schwenk, Phys. Rev. C **103**, 025803 (2021).
[41] W. Lynch and M. Tsang, Physics Letters B **830**, 137098 (2022).
[42] M. B. Tsang, Y. Zhang, P. Danielewicz, M. Famiano, Z. Li, W. G. Lynch, and A. W. Steiner, Phys. Rev. Lett. **102**, 122701 (2009).
[43] P. Morfouace, C. Tsang, Y. Zhang, W. Lynch, M. Tsang, D. Coupland, M. Youngs, Z. Chajecki, M. Famiano, T. Ghosh, G. Jhang, J. Lee, H. Liu, A. Sanetullaev, R. Showalter, and J. Winkelbauer, Physics Letters B **799**, 135045 (2019).
[44] B. A. Brown, Phys. Rev. Lett. **111**, 232502 (2013).
[45] M. Kortelainen, J. McDonnell, W. Nazarewicz, P.-G. Reinhard, J. Sarich, N. Schunck, M. V. Stoitsov, and S. M. Wild, Phys. Rev. C **85**, 024304 (2012).
[46] P. Danielewicz and J. Lee, Nuclear Physics A **922**, 1 (2014).
[47] Z. Zhang and L.-W. Chen, Phys. Rev. C **92**, 031301 (2015).
[48] B. T. Reed, F. J. Fattoyev, C. J. Horowitz, and J. Piekarewicz, Phys. Rev. Lett. **126**, 172503 (2021).
[49] E789_18 GANIL dataset , `https://doi.org/10.26143/ganil-2019-e789_18` (2019).